

## Research

# Multi-parameters approach to assessment of soil liquefaction vulnerability in wetland areas of Lagos, Southwestern, Nigeria

H. T. Oladunjoye<sup>1</sup> · K. S. Ishola<sup>2</sup> · K. F. Oyedele<sup>2</sup> · L. Adeoti<sup>2</sup>

Received: 24 September 2023 / Accepted: 24 January 2024

Published online: 02 February 2024

© The Author(s) 2024 [OPEN](#)

## Abstract

With respect to geology, most coastal terrains are underlain by problematic soils, some of which are liquefiable in nature and may cause sudden failure of engineering infrastructures. Against this background, this study was carried out to investigate the subsurface geology of some Lagos coastal areas and their engineering implications using geophysical and geotechnical methods. To achieve this purpose, the Multichannel Analysis of Surface Waves, Cone Penetration Test, and Standard Penetration Test were deployed. Surface waves measurements were collected using a 24-channel seismograph to which 4.5 Hz twenty-four vertical geophones were connected via the takeouts of the two cable reels. CPT soundings were carried out with a 10-tons motorized cone penetrometer and boring with SPT were carried out as well. The results of the Multichannel Analysis of Surface Waves measurements showed that the shear waves velocity ( $V_s$ ) ranges from 160 to 470 m/s. The very loose to loose sand delineated have  $V_s$  in the range from 170 to 250 m/s. The tip resistance and sleeve resistance values spanned between 4.0 and 72.0 kg/cm<sup>2</sup> and 6.0–94 kg/cm<sup>2</sup> respectively. The thickness of the liquefiable sands in the study area varied between 2.5 and 18.0 m. At Ikoyi site, owing to the prevalence of loose silty sand, corroborated by the available borehole data and the Liquefaction Potential Index, it is classified as having a high-risk liquefaction and could be responsible for the periodic damages to structural infrastructures such as roads and buildings. The sediments mapped at Okun-Ajah and Badore sites are mainly saturated loose sands with high likelihood to liquefaction with very-high to high risk severity. The study concludes that the presence of these sediments and other factors that could induce ground motion making the study sites potentially susceptible to liquefaction. Hence, an urgent attention must be given to early monitoring measures to address the trend.

## Article Highlights

- Study assesses use of electrical resistivity imaging and seismic refraction (via Multi Analysis Surface Waves) methods for near surface mapping/characterization
- The study sites belong to the wetland, coastal area of the Dahomey Basin, a part of sedimentary basin with sands deposits, peat, clay and their intercalation
- The shear waves velocity model integrated with CPT data proved to be useful tool for evaluation of soil liquefaction status with the index suggesting low–high–very high risks

**Keywords** Liquefaction · Earthtremors · Induced seismicity · Surface waves · Cone penetrometer test · Standard penetration test

---

✉ H. T. Oladunjoye, [oladunjoye.titilope@oouagoiwoye.edu.ng](mailto:oladunjoye.titilope@oouagoiwoye.edu.ng) | <sup>1</sup>Department of Physics, Olabisi Onabanjo University, Ago-Iwoye, Ogun State, Nigeria. <sup>2</sup>Department of Geosciences, University of Lagos, Akoka, Lagos, Nigeria.



## 1 Introduction

The major factors causing structural damage at the time of earthquakes have been identified as soil conditions, structural properties and earthquake characteristics [1, 2]. Earthquakes occurrence in Alaska, USA, and Niigata, Japan in 1964 have led to failures in the engineering structures owing to ground motion or vibrations [3]. In terms of geomorphology, both cities are situated on the coastal areas comprising alluvial sediments arising from deposition periods. Most of engineering structures have their founding layers on saturated cohesionless soil [3]. These events highlighted the problems associated with the saturated cohesionless soils during earthquake or seismic activities –whether natural or induced (caused by humans). Saturated loose granular sediments will experience a loss in bearing strength when subjected to rapid deforming load and might results in soil liquefaction; a phenomenon where a soil strength fails and behaves like a liquid [4]. Soil liquefaction may cause ground subsidence, settlements, sand boils, lateral spreading, slope failures and collapse of structures [5].

A review of past earthquakes/tremors suggests that structural failures are the common consequences of ground motion and individual seismicity [6, 7]. Several incidences of engineering constructions failures have been recorded in Nigeria, particularly in most major cities such as Lagos metropolis. Some of these structural failures have been linked to a number of factors including but not limited to the presence of peat/clay in the founding layer, use of inferior materials, and poor construction design among others [8]. In view of this, construction/structural engineers have adopted a method in which the construction of engineering designs are carried out on sandy layer, owing to its high bearing capacity characteristics. Consequent upon the adoption of this, the sandy layer has been proven to be the most competent founding soil for hosting the foundation footing of most engineering structures [8–11]. However, other studies have revealed that this cohesionless sandy soil is prone to liquefaction [12–14].

In Nigeria, history of the first seismic event was dated back to Earth tremors in Warri, South-south in 1933. This event was followed by another Earth tremor in Lagos in 1939 [15–17]. In 1961, ground movement reported in Ohafia was suggested to be due to lateral displacement rather than earth tremor [16, 18]. According to [15], the most severed tremors occurred in 1984 around Ijebu Ode, in Ogun State, southwestern, Nigeria. Other related studies in Nigeria have shown that about twenty earth tremors had been recorded between 2000 and 2007 [16, 19, 20]. Human daily activities such as indiscriminate abstraction of groundwater through boreholes and dredging activities around the coastal areas could possibly cause induced seismicity via deformation of the earth that could arise from stress and strain actions in the Earth's crust.

Despite that incidence of earth tremors have been recorded in Nigeria, Nigeria is not located on any of the active seismic plates [21]. The degree of damage to lives and properties caused by tremors vary in magnitudes, intensities and soil types. Even though induced seismicity had low magnitudes, they nevertheless have immense consequences on the bases of the damages caused to lives and properties. Based on the modified Mercalli Intensity Scale, the intensities of these events ranged from III (weak) to VI (strong) [17]. In scientific terms, it is noteworthy that some of these events were not documented due to non-availability of instrument at the time of their occurrences. Yet, the tremors recorded at Ijebu-Ode in 1984; Ibadan in 1990 and Jushi-Kwari in 2000 were due to body waves with magnitudes in the range of 4.3 to 5.5, 3.7 and 4.2, and surface waves of magnitudes 3.7 to 3.9 respectively [17].

However, assessment and mitigation measures for earthquakes have been suggested for induced seismicity [22]. Ref. [23] reported that the Dahomey Basin (of which the study area belongs) is associated with the equatorial fractures such as Romanche and Chain fracture Zones. These fracture zones are linked with the Gulf of Guinea and are reported to be responsible for the transportation of minerals and energy through the Atlantic Ocean [24]. Moreover, the Akwapim fault in Ghana, being one of the most active fault lines in Africa, also has a strong link with the Dahomey Basin, which enables the transportation of energy through the fault line [25, 26]. Elsewhere, preliminary investigations have shown that some of these tremors were due to different causes. They include unregulated mining activities, injection of water during oil and gas explorations. In Nigeria, areas where these activities are unabated might not be completely free from the consequences of induced seismicity.

In the light of the aforementioned, an attempt was made in this present study to provide a detailed understanding of the liquefaction potentiality of the Lagos coastal soils arising from induced seismic actions using the geophysical and geotechnical techniques. This is necessary because the coastal sands exhibit some characteristics that borders on the periods of deposition, degree of saturation, stratigraphic sequence, rate of compaction among others; all of which increases the proneness to liquefaction [27, 28]. The first part of this paper focuses on an insight into the occurrence of earth tremors; why they happened, their causes and effects. The second part presents a review of the

geological setting of the study area. Also, the different techniques used for the investigations, findings made and implications are presented.

## 2 Geological settings of the study area

The Lagos wetland belongs to the coastal plain sand formation of the Dahomey Basin [18, 29, 30]. As evident from Fig. 1, the Dahomey Basin is part of the coastal sedimentary basin in the Gulf of Guinea, extending from southeastern Ghana in the west to the western flank of the Niger Delta [29, 31]. The sequences of rock units from the youngest to the oldest, comprising the coastal plain sands, the Ilaro Formation, Oshosun Formation, Akimbo Formation, Ewekoro Formation, and Abeokuta Formation [29, 32]. The Precambrian Basement complex of Nigeria underlies the aforementioned Formations [33]. The age of coastal plain sands ranges from Pleistocene to Oligocene. The Litho-stratigraphic of the coastal plain sands reveals that it consists of unconsolidated dry and wet sand intercalated with clay deposits [18, 30, 32].

## 3 Materials and methods

For this study, the geophysical method of seismic refraction via Multichannel Analysis of Surface Waves (MASW) measurements from three sites the Badore, Okun—Ajah and Ikoyi along the Lagos coastal were carried out (Fig. 2). The geotechnical measurements carried out via the standard penetration tests (SPT N- values) from the drilled boreholes was performed by taking the N-values corresponding to the number of blows or blow counts. Also, the cone penetration tests (CPT) were performed by measuring the tip resistance ( $q_c$ ) of the cone to penetration. Furthermore, the shear-wave velocity ( $V_s$ ) data were used to evaluate the vulnerability of the coastal sands to liquefaction. The conditions for evaluating liquefaction resistance based on datasets from the shear wave velocity, SPT and CPT were available in the Cyclic Resistant Ratio (CRR) versus  $N_{1,60}$  plots [12]. The two steps taken in the evaluation of liquefaction potential were (i) delineation of lithologic units from the geophysical and geotechnical techniques and (ii) the estimation of Cyclic Stress Ratio (CSR), Cyclic Resistant Ratio (CRR) and the Factor of Safety (FS) for the geo-materials delineated. The CSR, otherwise known as the seismic demand on soil layer, represents the build-up of tremor occurrence. It explains the degree of demand that could be generated to initiate the likely seismic events on the geo-earth material. However, the evaluation of the site characteristics due to strain generated by CSR could also be used in the determination of the FS values. The CRR parameter was evaluated from the shear wave velocity ( $V_s$ ), cone tip resistance ( $q_c$ ), SPT N-values from the MASW CPT, and SPT techniques respectively.

**Fig. 1** Geology Map of Dahomey Basin [30]

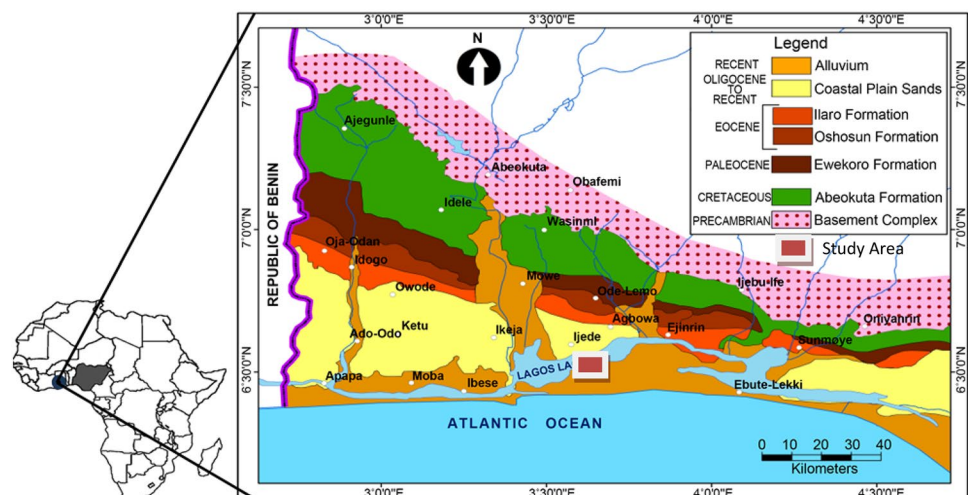
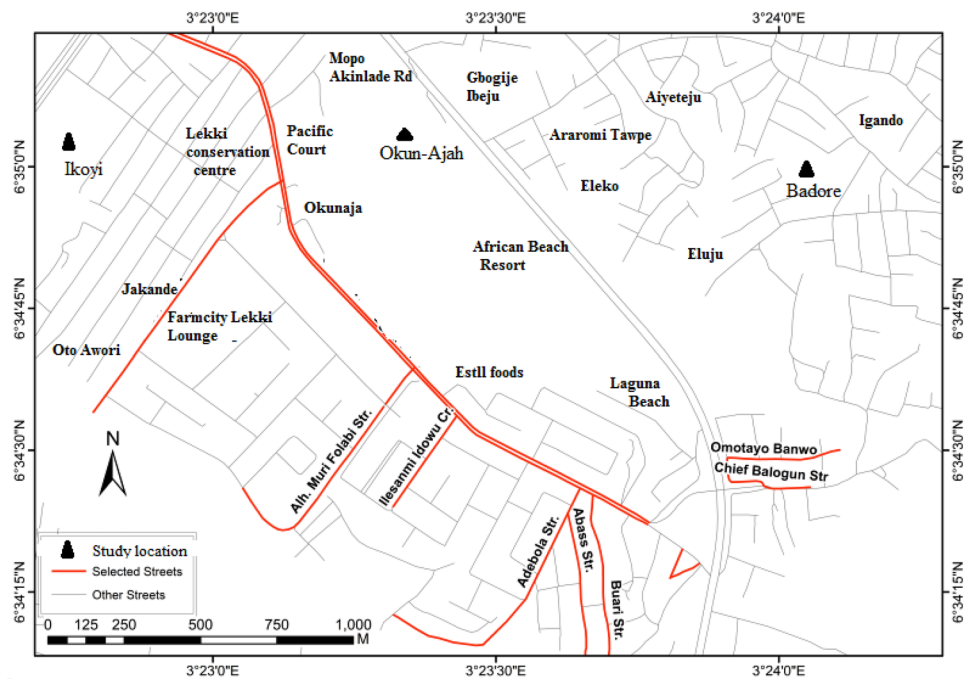


**Fig. 2** Base map of the study area showing the locations for surveys



### 3.1 Multi-channel analysis of surface waves measurements

The ground-roll configuration of Multi-channel Analysis of Surface Waves (MASW) technique [34, 35] was employed to produce the shear wave velocity ( $V_s$ ) profiles. The survey was carried out using a 24-channel ABEM Terraloc Mark 5 seismograph with 16 bit resolution. A set of 24 vertical geophones of frequency 4.5 Hz and a pre-trigger geophone connected to the seismograph via two cable reels each of length 100 m. Each of the cable reels consist of 24 take outs at fixed interval of 5 m. During the survey design, each of the self-orientating geophone was connected to one takeout and arranged in a linear array with geophone spacing between 3 and 5 m, depending on availability of space. The choice of the geophones intervals was to allow for optimum coverage of the study areas, allow observation of the near field effect, enhanced signals coherency and probing to a reasonable depth [11, 34]. The seismic waves were generated by sledge hammer which struck a square metal plate as a source of energy. The  $V_s$  profiles were calculated through an iterative inversion process using SeisImager software. The construction of dispersion curves was one of the critical steps taken for eventual generation of an accurate shear-wave velocity ( $V_s$ ) profile from back calculation of the  $V_s$  variation with depth from the extracted dispersion curves [21, 33].

### 3.2 Cone penetration tests measurements

Fifty CPT points were acquired within the wetland sites using a 10-Tons motorized Dutch cone penetrometer equipment due to its ability to measure the sleeve resistance, one of the liquefaction parameters. The penetration tests were carried out in accordance with the procedures in ASTM D-3441. The acquired CPT data were processed using NovoCPT following the steps contained in [11] and modified in [36, 37]. NovoCPT was designed not only to process the CPT data but also to perform interpretations of raw data in order to probe the soils behavior as well as estimate soil physical and mechanical properties. The cone tip resistance ( $q_c$ ) was normalized to a dimensionless cone penetration resistance ( $q_{c1N}$ ) using Eqs. 1 and 2.

$$q_{c1N} = C_Q \left( q_c / p_a \right), \quad (1)$$

$$C_Q = \left( P_a / \sigma'_{vo} \right)^n, \quad (2)$$

where:

$C_Q$  = normalizing factor for cone penetration resistance,

$P_a = 1$  atmospheric pressure in the same units used for  $\sigma_{v0}$ ,  
 $n =$  soil type exponent varies between 0.5—1.0 and.  
 $q_c =$  field cone penetration resistance measured at the tip.

### 3.3 Standard penetration tests (SPT) measurements

Seven boreholes were drilled at some strategic positions within the study areas with a view to knowing the soils stratigraphic sequence. The information obtained about the stratigraphic units was used in the classification of the geo-earth materials as either susceptible or non-susceptible units. The soil samples were collected using a split spoon sampler and necessary precautions were taken to avoid alteration of the soils conditions before laboratory analysis. The standard procedures described in [9] were adopted. The blow counts (N-values) needed to drive the sliding hammer into the soils, were recorded as the standard penetrating resistance. The N-values indicate the density of the ground [38]. The recorded N-values were corrected using the Eq. 3 for overburden pressure ( $C_N$ ), Hammer Energy ( $C_E$ ), Borehole Diameter ( $C_B$ ) Sample Liner, ( $C_S$ ) and Rod Length ( $C_R$ ) corrections. Table 1 gives the classification of the soils based on their N-values:

$$(N_1)_{60} = N \times C_N \times C_E \times C_B \times C_S \times C_R, \quad (3)$$

The CSR was estimated from the updated simplified procedure of [34] using Eq. 4

$$CSR = \frac{\tau_{av}}{\sigma'_{v0}} = 0.65 \frac{a_{max}}{g} \cdot \frac{\sigma_{v0}}{\sigma'_{v0}} \frac{MSF}{r_d}, \quad (4)$$

where:

$a_{max}$  = Maximum horizontal acceleration,  
 $\sigma_{v0}$  = Total vertical overburden stress,  
 $\sigma'_{v0}$  = Effective overburden stress,  
 $r_d$  = Stress reduction coefficient,  
 MSF = Magnitude Scaling Factor.  
 g = Acceleration due to gravity.

The Cyclic Resistant Ratio (CRR) describes the resistance of soils to liquefaction phenomenon. It was obtained from the shear wave velocity ( $V_s$ ) using Eq. 5.

$$CRR = a \left( \frac{V_{s1}}{100} \right)^2 + b \left( \frac{1}{V_{s1}^* - V_{s1}} - \frac{1}{V_{s1}^*} \right), \quad (5)$$

where:

$V_{s1}$  = Corrected shear wave velocity,  
 $V_{s1}^*$  = Limiting upper value of  $V_{s1}$ , a and b are curve fitting parameters.

The first incidence of earth tremor which occurred at Ijebu-Ode, southwestern Nigeria was recorded with an epi-centre intensity of about VI [26, 40]. Following this, a number of earth tremors have been witnessed with local magnitudes that span between 3.0 and 5.0 [20, 40, 41]. For the calculation of MSF relation proposed by [37], and  $M_w$  of 5.0 was used. The MSF was computed using Eq. 6

$$MSF = 10^{2.24} / M_w^{2.56}, \quad (6)$$

**Table 1** Classification of soil based on SPT-N values [39]

SPT (N- Value)	Classification
0–4	Very loose
4–10	Loose
10–30	Medium dense
30–50	Dense
> 50	Very dense

The liquefaction empirical relationships involve the estimation of CRR against liquefaction from the corrected  $(N_1)_{60}$ . This is presented in Eq. 7 as updated by [37].

$$CRR = \exp \left\{ \frac{(N_1)_{60cs}}{14.1} + \left( \frac{(N_1)_{60cs}}{126} \right)^2 - \left( \frac{(N_1)_{60cs}}{23.6} \right)^3 + \left( \frac{(N_1)_{60cs}}{25.4} \right)^4 - 2.8 \right\}, \tag{7}$$

A Factor of Safety (FS) expressed as ratio of CRR to CSR was computed using Eq. 8. Liquefaction is expected to trigger when  $FS < 1$  (unity)

$$F_s = \frac{CRR}{CSR}; F_s < 1.0 = \text{Liquefaction}, \tag{8}$$

### 3.4 Liquefaction potential index

Liquefaction Potential Index (LPI) estimates the severity of liquefaction potential phenomenon. This parameter complements the severity obtained from the FS. LPI is important because the FS values against soil liquefaction might not be sufficient for the evaluation of the severity of liquefaction [42]. A soil layer with  $FS > 1$  is classified as liquefiable. According to [43], FS values of 1.0 and 1.2 are defined as non-liquefiable and marginally liquefiable layers respectively. Hence, LPI incorporates the depth and thickness of the liquefiable layer with FS in evaluating the liquefaction severity. The thicker a liquefiable soil layer is the more severe it is to liquefaction. The LPI model proposed by [44] in Eq. 9 was used to estimate the severity of the soil to liquefaction.

$$LPI = \int_0^{20} (10 - 0.5z) \times F_L \times d_z, \tag{9}$$

The conditions for evaluating the  $F_L$  are presented in Eqs. 10 and 11:

$$F_L = 1 - FS; FS < 1, \tag{10}$$

$$F_L = 0; FS > 1, \tag{11}$$

Four discrete liquefaction severity categories proposed by [44] based on numerical values of LPI are indicated in Table 2. Liquefaction effects are moderate for  $5 < LPI < 15$  and major for  $LPI > 15$  with the consequences of sand boils to a total loss of bearing capacity.

**Table 2** Locations with depths, SPT N- values, CRR, CSR, FS, and vulnerability status

Location	Depth (m)	SPT "N" Value	CRR	CSR	FS	Vulnerability status
Okun-Ajah	0.0–2.3	15–20	0.148–0.168	0.139–0.140	1.06–1.20	No
	2.3–15.0	3–10	0.075–0.156	0.172–0.230	0.34–0.86	Yes
	15.0–22.5	18–26	0.192–4.000	0.162–2.000	1.19–2.00	No
Badore	0.0–3.0	12–18	0.165–0.290	0.139–0.196	1.18–1.48	No
	3.0–17.0	3–12	0.070–0.111	0.182–0.230	0.32–0.61	Yes
	17.0–21.0	18–30	0.148–0.268	0.165–0.171	1.00–1.63	No
Ikoyi	0.0–3.0	28–30	0.224–0.374	0.187–0.189	1.20–1.97	No
	3.0–6.3	10–17	0.118–0.206	0.230–0.244	0.49–0.90	Yes
	6.3–25.0	18–26	0.165–0.555	0.147–0.231	1.12–2.00	No

### 4 Results and discussion

The N-values results of SPT measurements presented as profiles obtained for the three locations; the Okun-Ajah, Badore and Ikoyi are shown in Fig. 3a–c. The N-values used for the borehole logs classification (the stratigraphic sequence) at each sounding point is presented in Table 1. In Fig. 3a, the SPT log obtained for Okun–Ajah location shows that the stratigraphic units range from medium grained coarse sand–loose silty sand to very loose sand with an average depth of 22 m. The topsoil is medium grained coarse sand with N-values between 18 and 20 at depth 2.5 m from the ground surface. It is noticed that beneath this layer, loose silty sand with N-values between 9 and 15 at depth that spans between 2.5 and 5 m is encountered. Also, at depth between 5 and 10 m, loose sand with N-values that spans between 3 and 6 is encountered. The sediment encountered at depth range of 10 – 15 m with N-values between 7 and 10 is presumably loose silty sand. Next, a medium to dense coarse sand is encountered at a depth of about 15 m till the end of the borehole. The corresponding N-values are in the range of 16–35. Thus, liquefiable sediments are observed at depth between 2.5 and 15 m with N-values that span between 3 and 10. However, the vulnerability of the silty sediments depends on the degree of fine particles present.

The SPT profile for Badore site shown in Fig. 3b suggests that liquefiable sediments are encountered at depth between 3 m and 17.5 m. These sediments correspond to loose sands – loose silty sand with SPT “N” values between 3 and 12. The very loose sand sediments are potentially susceptible to liquefaction [4]. Also, Fig. 3c is the borehole log data at Ikoyi site loose silty sands with SPT “N” values between 9 and 14 at depth values of 5–10 m are encountered.

Table 2 gives a range of FS values as the function of the depth obtained from the empirical relation and SPT N-values. At Badore site, loose silty sand and very loose sand with the FS values in the range of 0.32 and 0.61 and depth between 3 and 17 m are encountered. Since the sediments are classified as low, they are more vulnerable to liquefaction. At Okun—Ajah site, the computed FS values span between 0.34 and 0.86 with depth between 2.3 and 15.0 m with SPT N-value ranging from 3 to 10. At Ikoyi site, the silty sediments delineated at depth between 3 – 6.3 m have FS values between 0.49 and 0.90. The silty sand sediments classified as highly liquefiable are suspected saturated with fluid.

Table 2 Summary of locations with depths, SPT N- values, CRR, CSR, FS and vulnerability status.

The results of MASW measurements are presented in two folds as: (i) delineated stratigraphic sequence and (ii) evaluation of liquefaction potential of the areas using the Factor of Safety (FS) values. The stratigraphic sequence provides information regarding the composition and arrangement of the layers. This helps to classify sediments delineated on the basis of their shear wave velocities (Vs). The two-dimensional (2D) Vs models for the three sites are shown in Fig. 4. In Fig. 4a, the Vs spans between 170 and 263 m/s. For the topsoil, the Vs ranges from 234 to 261 m/s; depth between 0 and 3 m. This layer connotes silty—very loose—medium dense sand. Beneath the topsoil is medium dense silty sand with Vs

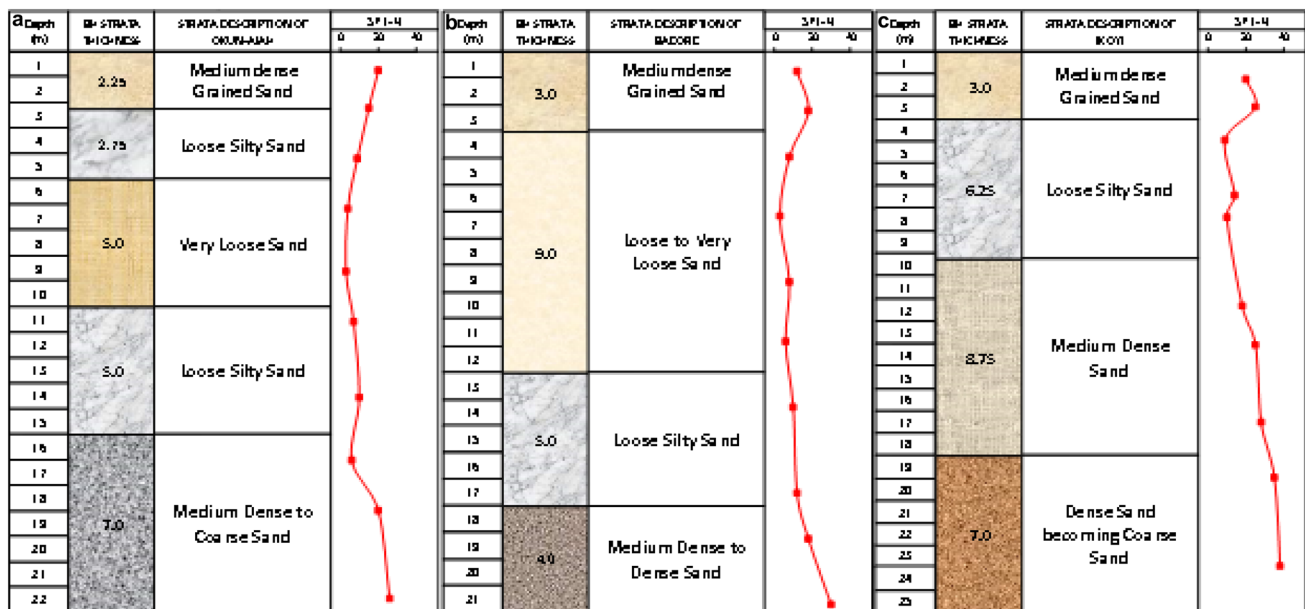
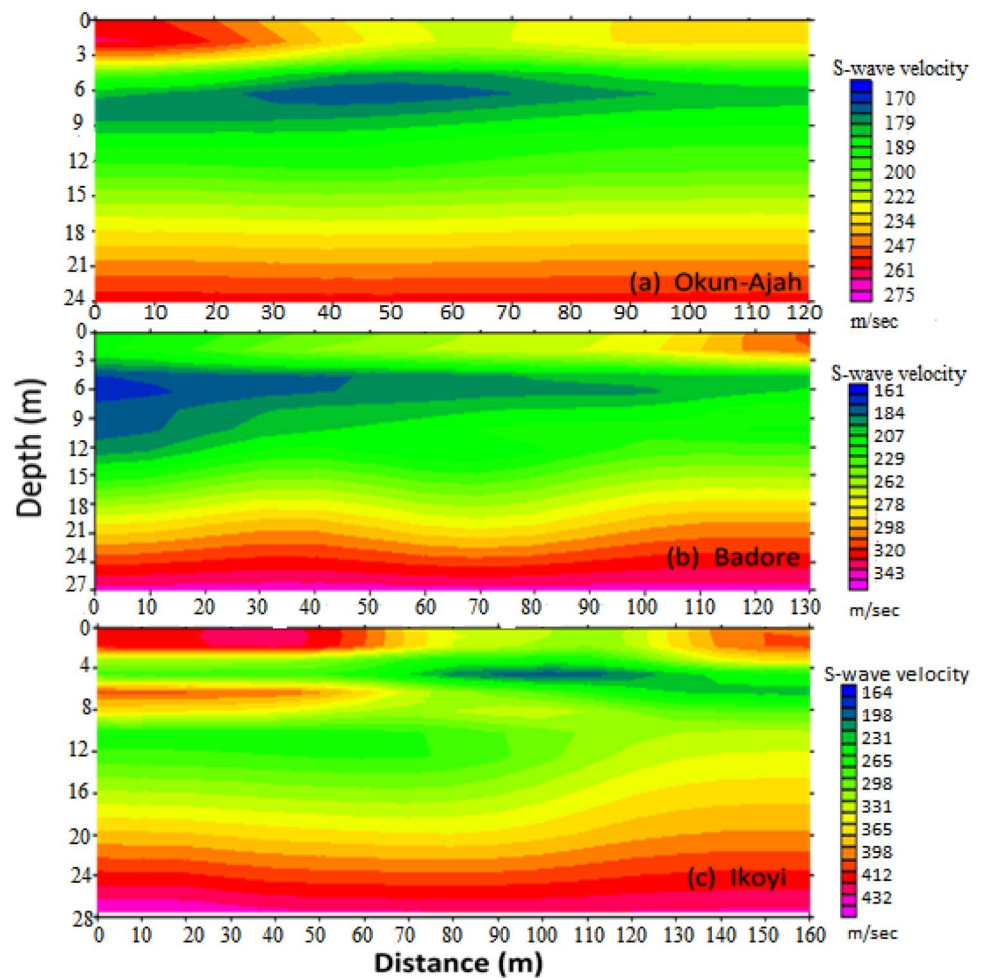


Fig. 3 SPT profiles obtained at one of the borehole sites for (a) Okun-Ajah (b), Badore (c) Ikoyi (d) Ikoyi

**Fig. 4** 2D shear wave velocity models for the three sites



between 190 and 211 m/s at a depth of 3–6.0 m. Also, loose sand at depths of about 6–9.0 m, with  $V_s$  values of between 175 and 185 m/s is delineated. At depth between 10 and 18 m, silty sand with  $V_s$  values of 200 and 230 m/s is mapped. It is clearly seen that at deepest portion of the velocity model (18.0 and 24.0 m), a layer made of dense soil with  $V_s$  ranging from 235 to 260 m/s is demarcated. The ranges of values for  $V_s$  in this study are in consonance with similar studies conducted by [11, 45, 46] [47] reported that for liquefiable soils, the  $V_s$  lies between 100 and 250 m/s. On this backdrop, the third lithological unit that comprises of loose sand is probable the liquefiable sediments at Okun-Ajah site. Similarly, the second and fourth lithological units are the possible liquefiable regions although their vulnerability to liquefaction is low compared to the loose-sand. Figure 4b is the 2D  $V_s$  model at the Badore site with velocity distribution between 161 and 366 m/s. The topsoil has  $V_s$  that ranges from 229 to 302 m/s with an average thickness of about 3 m. It is clearly noticed that beneath this layer, saturated loose sand at depth range of 3.1–13.5 m and  $V_s$  values that span between 161 and 204.0 m/s is mapped. Furthermore, this layer is underlain by silty sand with  $V_s$  values of 210 and 275 m/s and a depth in the range of 16–21.5 m, representing the third lithological layer of this profile. The fourth lithologic layer comprises medium dense sand, with  $V_s$  values varying between 320 and 366 m/s; its corresponding depth value ranges between 21 and 27 m. This finding is in agreement with the results of [46]. Thus, the second lithologic layer made of saturated loose sand is suspected to have high potentiality to liquefaction. The 2D  $V_s$  model for Ikoyi site is shown in Fig. 4c. It shows that the ground structure consists of three lithological units with variation from loose and medium dense sand. For this model, the  $V_s$  ranges from 161 to 231 m/s (blue); 231–331 m/s (greenish–yellow), 331–465 m/s (red). The topsoil has  $V_s$  that lie between 435 and 350 m/s with an average thickness of 3 m from the ground surface. The second lithologic layer is made of loose silty layer at depth of 3 to 8 m; the  $V_s$  values of span between 168 and 230 m/s. The degree of susceptibility of the delineated soils depends on the percentage of fine particles within the soils sample [48]. Thus, a significant part of the velocity model is prone to liquefaction since the  $V_s$  falls within the classification scheme of [47].



**Fig. 5** CRR curve obtained from the shear wave velocity at (a) Okun-Ajah (b) Badore and (c) Ikoyi sites

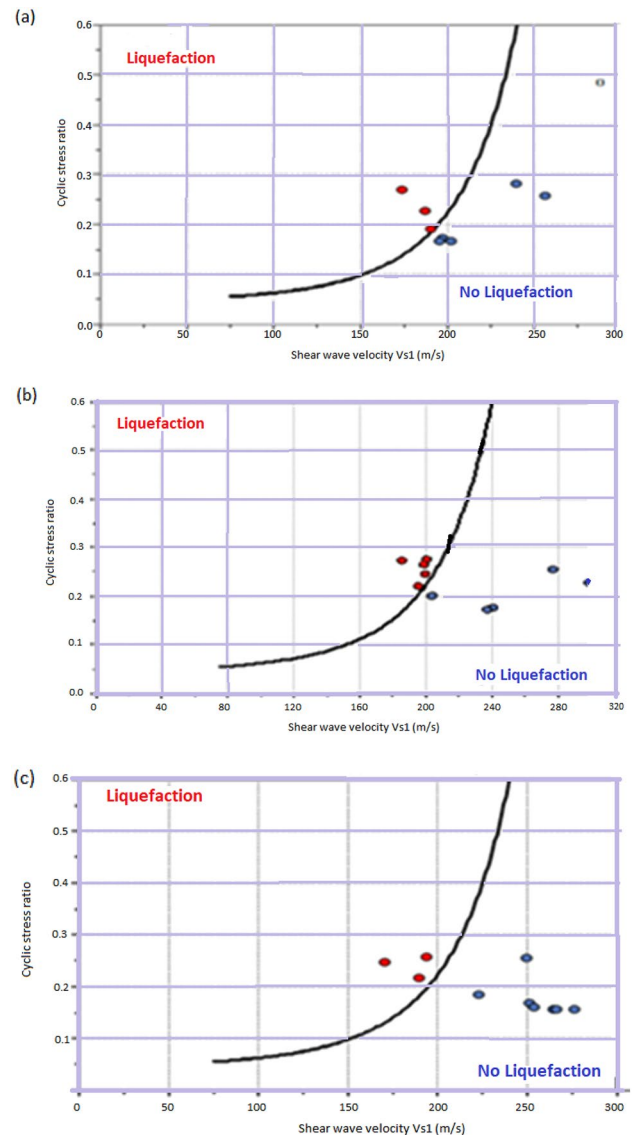


Figure 5a–c is the CRR-curve that shows the liquefaction resistance boundaries where liquefaction may likely occur or not. In Table 2, the liquefiable points at Okun—Ajah are within the depths of 2.25–15.0 m, while the FS values vary from 0.34 to 0.86 (i.e., less than 1). The geological materials at these depths consist of very loose–loose sand. Based on the FS values, the potential hazard zone occurs at 9 m from the ground surface to an average depth of about 18 m. In Fig. 5b, the CRR-curve for Badore site with FS values between 0.62 and 0.93, an indication that possible liquefiable layers could be encountered at between 5.0 and 12.0 m. At Ikoyi site, pockets of layer (in the form of sand sediments) prone to liquefaction are delineated. Furthermore, at depth of between 5 and 10 m, liquefiable layers with FS values that span between 0.52 and 0.82 are delineated.

The CPT soundings results are presented as the cross plots of: (i) cone tip penetration resistance; (ii) Factor of safety (FS); (iii) probability plots and (iv) soil classification charts for Ikoyi (Fig. 6), Okun–Ajah (Fig. 7), and Badore (Fig. 8) respectively. The cone tip resistance plot determines the shear strength of the soil [46]. The engineering properties of the soils such as shear strengths are further expressed as the soil classification plots. The soil classification charts show a detailed description of the different sand constituents from the CPT data. The FS plots give information about the depths of liquefiable sediments at all the sounded points while the probability plots (PP-plots) show the possibility of unearthing liquefiable sediments at any depths [12]. The PP-plots show an inverse relationship with the FS plot. As the FS tend to 1 (i.e., an indication of the presence of non-liquefiable sediments), the probability plot approaches zero. The total cone tip penetration resistance plot shows the presence of materials

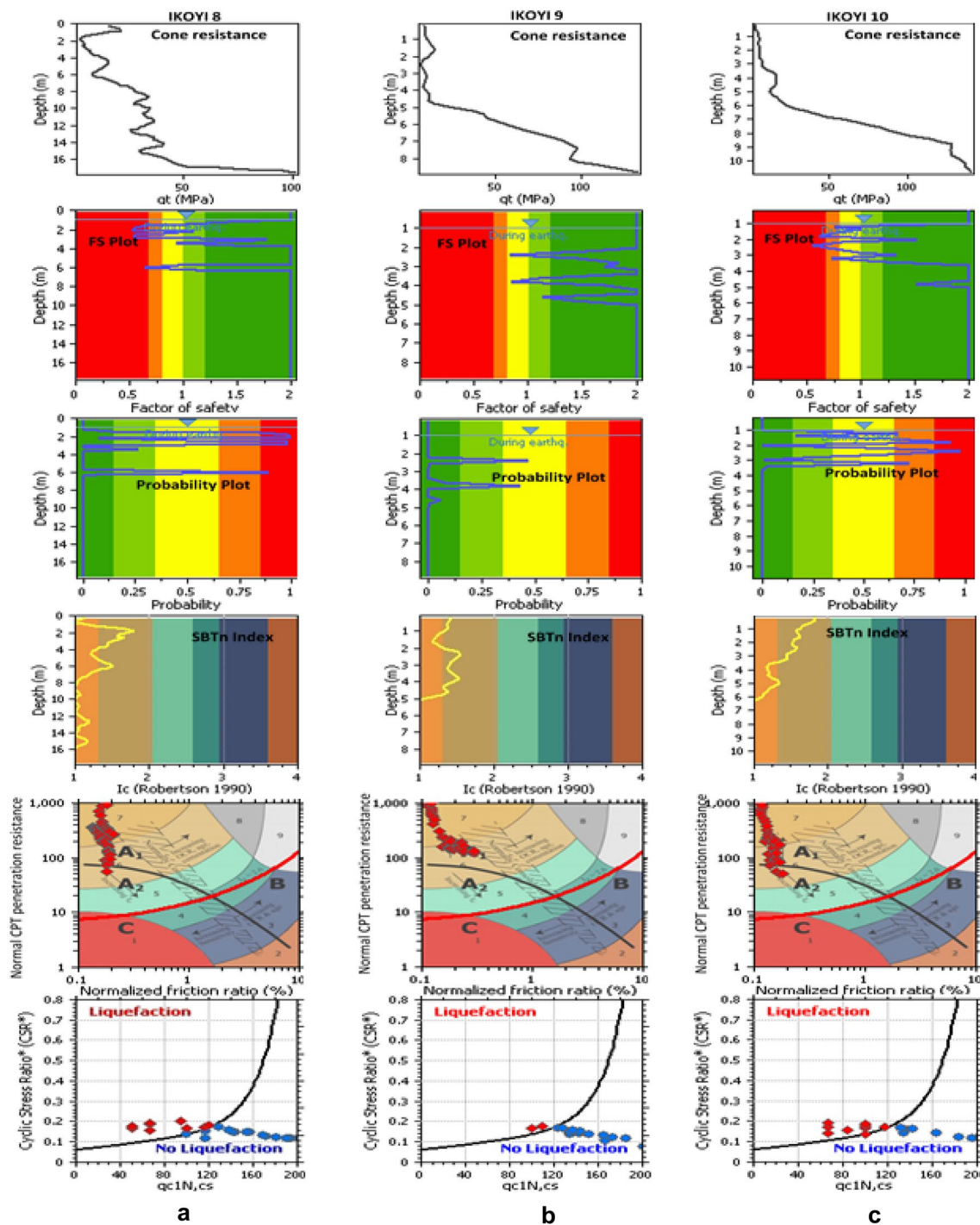


Fig. 6 CPT results in three locations at Ikoyi for (a) cone resistance (b) FS (c) liquefaction potential

with low shear strength at shallow depths 6 m from the ground surface. Figure 6 (IKY8) reveals that the topsoil, with an average thickness of 2 m, exhibits a low load resistance of about 30 kg/cm<sup>2</sup> suggesting loose silty sediments. Loose silty sediment with fluid contents is encountered at a depth in the range of 2–6 m; the corresponding cone resistance values lie between 2 and 30 kg/cm<sup>2</sup>. These values agree with the results of the CPT obtained at another located in the wetland area [46]. At depth between 6 and 14 m, geo-materials that have medium resistance of about 30–50 kg/cm<sup>2</sup> are encountered while beyond 14 m, the geo-materials have cone resistance of more than 50 kg/cm<sup>2</sup>. The FS plot of Fig. 6b shows the presence of liquefiable layer of within the depth values of 2–6 m; with FS values

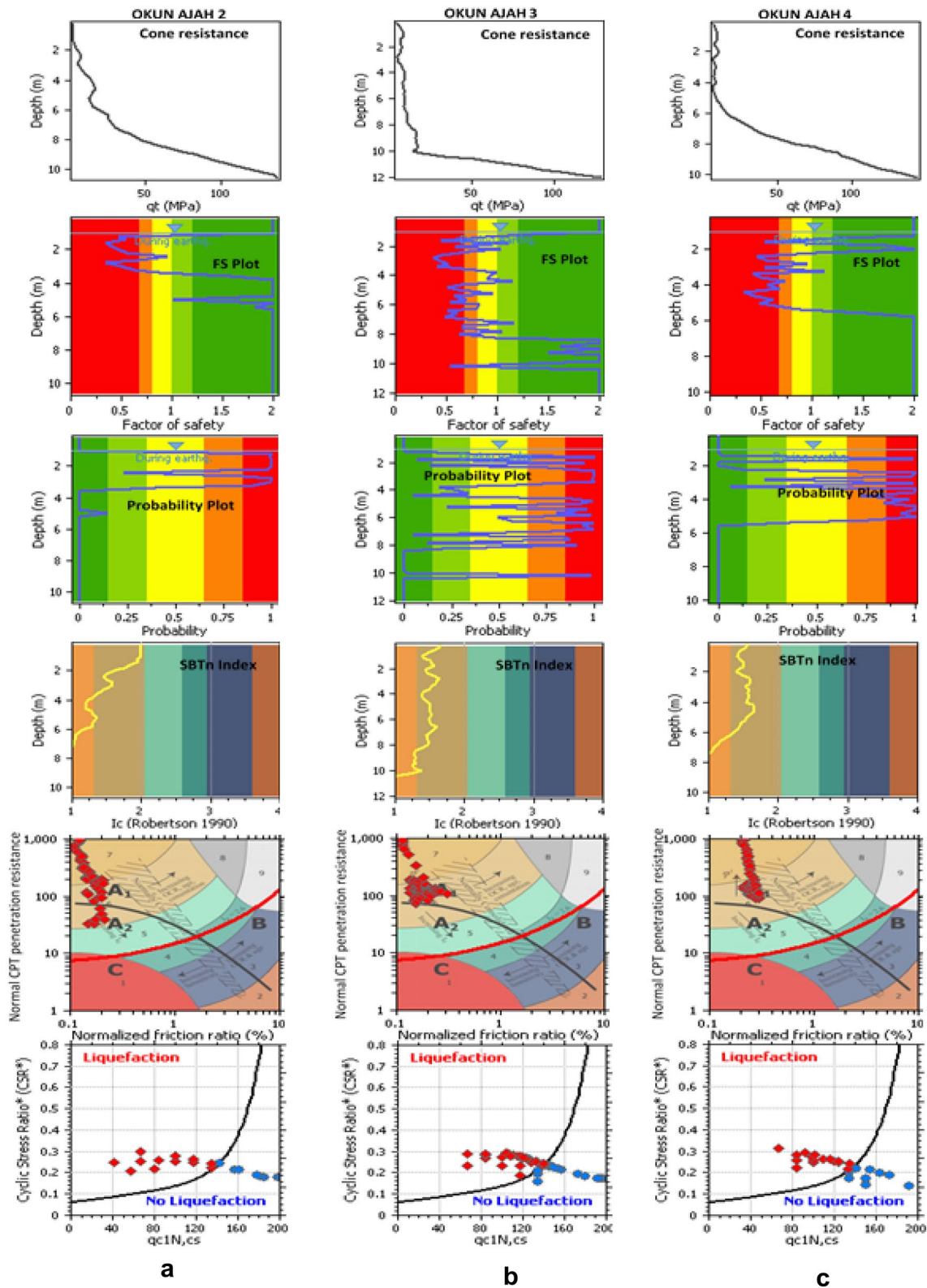


Fig. 7 CPT results in three locations at Okun-Ajah for (a) cone resistance (b) FS (c) liquefaction potential

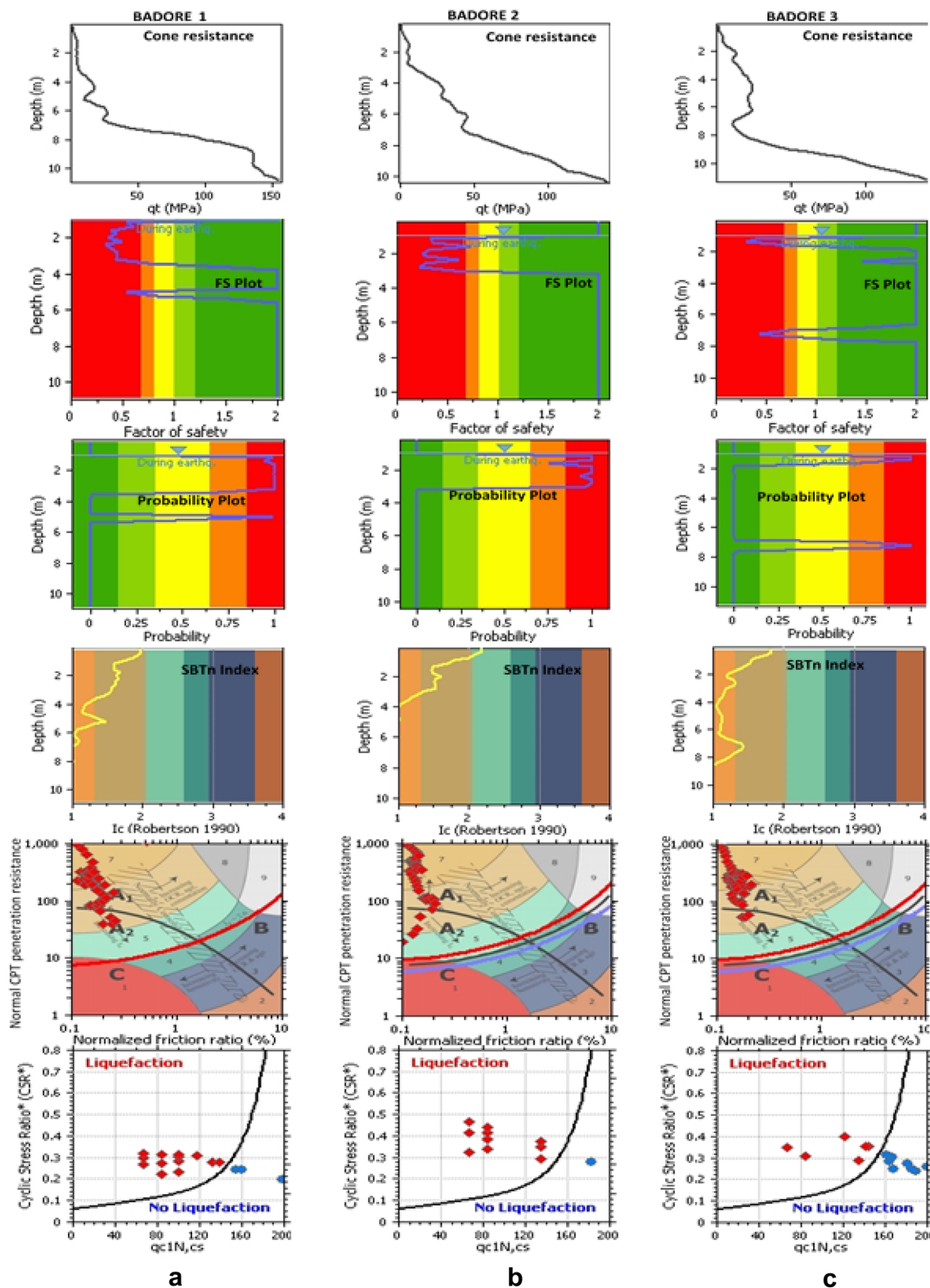
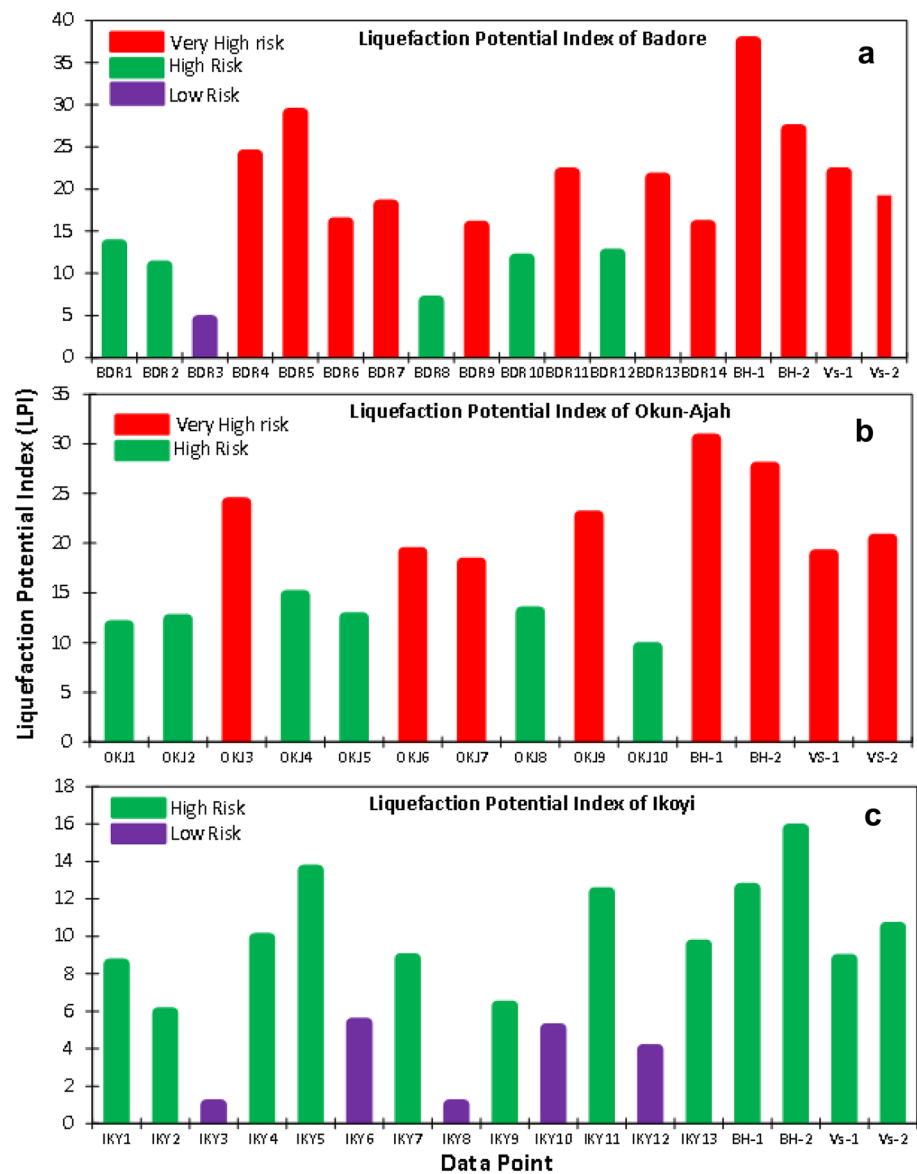


Fig. 8 CPT results in three locations at Badore for (a) cone resistance (b) FS (c) liquefaction potential

of between 0.5 and 0.9. The FS value increases to about 2.0 (representing safe sediments against liquefaction) at a depth of about 6 m to the end of the sounding point. It is also observed that at a depth of between 2 and 6 m, the probability plot (PP) approaches 1, suggesting a high likelihood for sand liquefaction to take place. The PP-plot

**Fig. 9** Histogram of the Liquefaction Potential Index with boreholes for (a) Badore (b) Ajah—Okun, (c) Ikoyi



approaches zero as the depth increases from 6 to 14 m. This indicates that the layer/zone is stable and not prone to liquefaction. In addition, the soil classification chart shows that the soil sediments encountered comprises of sand of various grades (i.e., dense, clean, silty sands) with very low normalized friction ratio. Similarly, at three sites in Ikoyi tagged IKY9, IKY10 and IKY11, liquefiable sediments are observed at depths between 2.5 and 5 m, 1.8–3.2 m and 2.0–3.5 m respectively. The estimated cone tip resistances at these depths span between 5 and 45 kg/cm<sup>2</sup>, 5–20 kg/cm<sup>2</sup> and 10–50 kg/cm<sup>2</sup> respectively. Also, the FS values are between 0.7 and 0.9, 0.3–0.5, and 0.6–0.9 while the PP-plots are 0.8–1.0, 0.6–0.9, and 0.5–1.0 respectively. It follows from the estimated parameters that Ikoyi site at average depth of about 2.5 m, liquefiable sediments are more likely to be encountered. The results at Okun–Ajah site, tagged OKJ1, OKJ2, OKJ3, and OKJ4, are shown in Fig. 7a–c. It reveals that liquefiable sediments are possibly encountered at depths ranging from 2.0 to 10 m (OKJ1), 2.0–8 m (OKJ2), 2.0–5.8 m (OKJ3) and 1.8–6 m (OKJ4). Furthermore, within these depths range, the FS and PP values are 0.4–0.9 and 0.5–1.00; 0.5–0.9 and 0.4–1.0; 0.3–0.7 and 0.65–1.0; 0.45–0.9 and 0.5–1.0 respectively. At the Badore site (Fig. 8a–c), the locations are tagged BDR1, BDR2 and BDR3, the liquefiable sediments are delineated at depths range of 1.6–6 m, 1.8–5.8 m and 1.8–12.5 m respectively. The estimated FS and PP values are 0.3 – 0.7 and 0.75–1.0; 0.25–0.9 and 0.6–1.0; 0.4–0.8, and 0.75–1.0 respectively. Both at Okun–Ajah and Badore, the lithological units delineated are mainly sands with varying grades due to the presence of silt making the silty sand liquefiable. The soil classification plots show that the sand sediments have

**Table 3** Liquefaction potential severity classification [44]

LPI Values	Severity classification
0	Very low risk
0.1–4.9	Low risk
5.0–14.9	High risk
15.0–100	Very high risk

normalized friction ratio less than 1% suggesting that fine content in the sediments are low and predominantly cohesionless. In general, it is clearly observed that the depth of possible liquefiable sediments at Ikoyi seems to be most shallow when compared to sediments at Okun-Ajah and Badore sites. This might be due to the degree of compaction the soil sediments at Ikoyi could have undergone. Similarly, the different thickness and vulnerability to liquefaction recorded at Okun-Ajah and Badore could possibly be due to fluid saturation arising from proximity to water bodies of the Atlantic Ocean and Lagos Lagoon respectively.

LPI measure the degree of liquefaction severity posed at each sounding point. The degree of severity is classified as 'low', 'high' or 'very high' based on the LPI values obtained at each sounding point according to the classification schemes of [44, 50]. The consequences of low, high or very high LPI values manifest as sand boils, lower settlement, minute lateral displacement and total bearing capacity [13]. The estimated LPI for the study areas, in terms of the degree of severities to liquefaction potential is illustrated with histograms in Fig. 9a–c. For the Badore site (Fig. 9a), the LPI values are in the range of 4.4–37.5. With this range, the site is classified as having low, high and very high-risk LPI [50]. These values indicate that high to very high risks liquefaction severity could occur as lateral displacement (settlement) owing to loss of bearing capacity. Hence, the site is not suitable for massive engineering structural development and periodic monitoring of the seismic events in the area becomes necessary. Similarly, the LPI at the Okun-Ajah site (Fig. 9b), ranges from 9.5 to 30.5 indicating a high to very-high LPI while at Ikoyi site, the LPI lies between 1.0 and 13.5 indicating that the area is susceptible to liquefaction severity and is therefore classified as either low or high (Table 3) [45, 50]. These points to the fact that the expected degree of liquefaction severity varies from one location to the other. The Badore and Okun—Ajah sites demonstrate high to very high risks while the Ikoyi site indicates that its potentiality to liquefaction severity is classified as low to high risk. The lithologic units delineated at Badore and Okun—Ajah suggest that the sites contain more recent sediments as a result of the recent reclamation of the locations with alluvial sands [18, 50, 50]. This means that the recent age of these materials might have contributed to the lofty increase in the estimated LPI. Conversely, the geo-earth materials observed at Ikoyi site, with some degrees of vulnerability to liquefaction, appears to have undergone different stages of compaction due to age. The sediments are less saturated, making them less vulnerable to liquefaction when compared to Badore and Okun- Ajah locations due to their proximity to the Lagos Lagoon and Atlantic Oceans respectively. Despite the low-risk potential at Ikoyi, the dominance of the high risk LPI and the borehole data analysis suggest that the area is prone to liquefaction.

## 5 Conclusions

Soil potentiality to liquefaction that could arise from induced seismic activities in some locations around Lagos coastal plain has been investigated using parameters estimated/derived from both geophysical and geotechnical techniques. The study revealed that the delineated coastal sands in Badore, Okun-Ajah and Ikoyi sites are vulnerable to liquefaction with varying severity. The sediments are of low shear strength and encountered at shallow depth with an average of 8 m. In some cases, the Badore and Okun-Ajah sites both exhibit saturated loose sands up to a depth of about 18 m. The study also shows that these sediments vary from very loose to saturated silty sands with the presence of very few fine particles, even as the thickness of the liquefiable sediments observed at Ikoyi suggests the presence of loose silty sand that has undergone compaction. This demonstrates mild susceptibility to liquefaction. Despite the delineated loose silty sand at Ikoyi, the dominance of the high-risk LPI and the borehole data analysis suggest that the area is prone to liquefaction and that damage to engineering infrastructures is more probable. The sediments at both Okun- Ajah and Badore are mainly loose sand with measure of saturation illustrating a high degree of liquefaction vulnerability, thus, it is grouped as high to very-high severity risk. The severity of occurrence generally increases with an increase in the LPI. The presence of these sediments with the several factors that could

induced seismicity make the study area more vulnerable and requires urgent monitoring measures. Since geology gives a clue to the future, it is expected that minor earthquake or earth tremors would continue to take place, it is therefore expected to continue to monitor those activities that could potentially trigger earthquakes via densifications of seismic stations and integration with Global Positioning System stations. Hence, in the future study, seismic hazard mitigation based on vulnerability index estimation is proposed.

**Author contributions** HTO carried out the data collection, processing data and preparations of manuscript KSI involved in data collection and preparation of manuscript KFO conceived and designed the research as well as supervision LA supervised the research and give technical support.

**Funding** The authors have not disclosed any funding.

**Data availability** All authors agree that the data used in this study are primary data collected by the authors with the assistance of our technologists and field assistance. However, we shall make the data used available to anyone on request.

## Declarations

**Competing interests** None.

**Open Access** This article is licensed under a Creative Commons Attribution 4.0 International License, which permits use, sharing, adaptation, distribution and reproduction in any medium or format, as long as you give appropriate credit to the original author(s) and the source, provide a link to the Creative Commons licence, and indicate if changes were made. The images or other third party material in this article are included in the article's Creative Commons licence, unless indicated otherwise in a credit line to the material. If material is not included in the article's Creative Commons licence and your intended use is not permitted by statutory regulation or exceeds the permitted use, you will need to obtain permission directly from the copyright holder. To view a copy of this licence, visit <http://creativecommons.org/licenses/by/4.0/>.

## References

1. Ansal A, Akinci A, Cultrera G, Erdik M, Pessina V, Tönük G, Ameri G. Loss estimation in Istanbul based on deterministic earthquake scenarios of the Marmara Sea region (Turkey). *Soil Dyn Earthq Eng*. 2009;29(4):699–709. <https://doi.org/10.1016/j.soildyn.2008.07.006>.
2. Akkaya İ. Availability of seismic vulnerability index (K<sub>g</sub>) in the assessment of building damage in Van, Eastern Turkey. *Earthq Eng Eng Vib*. 2020;19:189–204. <https://doi.org/10.1007/s11803-020-0556-z>.
3. Housner, G.W. (1985) Liquefaction of Soils during Earthquakes. Report by the Committee on Earthquake Engineering, Commission on Engineering and Technical Systems, National Research Council. National Academy Press.
4. Thevanayagam S, Martin GR. Liquefaction in silty soils screening and remediation issues. *Soil Dyn Earthquake Eng*. 2002;22:1035–42. [https://doi.org/10.1016/S0267-7261\(02\)00128-8](https://doi.org/10.1016/S0267-7261(02)00128-8).
5. Porcino DD, Tomasello G. Shear wave velocity-based evaluation of liquefaction resistance for calcareous sands of different origin. *Soil Dyn Earthq Eng*. 2019;122:235–47. <https://doi.org/10.1016/j.soildyn.2019.03.019>.
6. Marcusson WF. Definition of terms related to liquefaction. *J Geotech Eng Div*. 1978;104:1197–2000. <https://doi.org/10.1061/AJGEB6.0000688>.
7. Toprak S, Holzer T. Liquefaction potential index: field assessment. *J Geotech Geoenviron Eng*. 2003;129:315–22. [https://doi.org/10.1061/\(ASCE\)1090-0241\(2003\)129:4\(315\)](https://doi.org/10.1061/(ASCE)1090-0241(2003)129:4(315)).
8. Ayolabi EA, Enoch IJ, Folorunso AF. Engineering site characterization using 2-D and 3-D electrical resistivity tomography. *Earth Sci Rev*. 2013;2:133–42. <https://doi.org/10.5539/esr.v2n1p133>.
9. Adeoti L, Ojo AO, Adegbola RB, Fasakin OO. Geoelectric assessment as an aid to geotechnical investigation at a proposed residential development site in Ilubirin, Lagos. *Southwestern Nigeria Arabian J Geosci*. 2016;95:338. <https://doi.org/10.1007/s12517-016-2334-9>.
10. Adiat KAN, Akinlalu AA, Adegoroye AA. Evaluation of road failure vulnerability section through integrated geophysical and geotechnical studies. *NRIAG J Astron Geophys*. 2017;6:244–55. <https://doi.org/10.1016/j.nrjag.2017.04.006>.
11. Uwaezuoke CC, Ishola KS, Ayolabi EA. Electrical resistivity imaging and multichannel analysis of surface waves for mapping the subsurface of a wetland area of Lagos, Nigeria. *NRIAG J Astron Geophys*. 2021;10(1):300–19. <https://doi.org/10.1080/20909977.2021.1927427>.
12. Youd TL, Idriss IM, Andrus RD, et al. Liquefaction resistance of soils: summary report from the 1996 NCEER and 1998 NCEER/NSF workshops on evaluation of liquefaction resistance of soils. *J Geotech Geoenviron Eng ASCE*. 2001;127:297–313.
13. Rahman MZ, Siddiqua S. Evaluation of liquefaction-resistance of soils using standard penetration test, cone penetration test, and shear-wave velocity data for Dhaka, Chittagong, and Sylhet cities in Bangladesh. *Environ Earth Sci*. 2017;76:207. <https://doi.org/10.1007/s12665-017-6533-9>.
14. El Hilali M, Timoulali Y, Benyounes T, Ahniche M, El Bardai R, Yattara S. Earthquake-induced liquefaction in the coastal zone, Case of Martil city, Morocco. *E3S Web of Conferences*. 2021; 298, 01002 (2021). <https://doi.org/10.1051/e3sconf/202129801002>
15. Ajakaiye DE. Earthquakes – What are they? In *Proceedings of the National Seminar on earthquakes in Nigeria* (Ed.) Ajakaiye D. E; Ojo S. B. and Daniyan M. A.5 – 42. 1989.
16. Eze CL. Tsunami: facts and figures for Nigerian Coastal Dwellers and Tourists. *Transparent Earth Nigeria Limited*. 2007.
17. Akpan UO, Yakubu TA. A review of earthquake occurrences and observation in Nigeria. *Earthq Sci*. 2010;23:289–94. <https://doi.org/10.1007/s11589-010-0725-7>.
18. Adepelumi AA, Olorunfemi MO. Engineering geological and geophysical investigation of the reclaimed Lekki Peninsula, Lagos. *South West Nigeria. Bull Eng Geol Env*. 2000;58:125–32. <https://doi.org/10.1007/s100640050006>.

19. Osagie EO. Seismic activity in Nigeria. *The Pac Jour Sci & Tech.* 2008;9(2):1–6.
20. Akpan OU, Isogun MA, Yakubu TA, Adepelumi AA, Okereke CS, Oniku AS, Oden MI. An evaluation of the 11th september, 2009 earthquake and its implication for understanding the seismotectonics of South Western Nigeria. *Open J Geol.* 2014;4:542–50.
21. Adepelumi AA, Yakubu TA, Alao OA, Adebayo AY. Site dependence earthquake spectra attenuation modeling: Nigerian case study. *Int J Geosci.* 2011;2:549–61. <https://doi.org/10.4236/ijg.2011.24058>.
22. Mignan A, Landtwing D, Kästli P, et al. Induced seismicity risk analysis of the 2006 Basel, Switzerland, enhanced geothermal system project: Influence of uncertainties on risk mitigation. *Geothermics.* 2015;53:133–46. <https://doi.org/10.1016/j.geothermics.2014.05.007>.
23. Samaila NK, Likkason OK. Role of equatorial fracture zones on fluid migration across the South Atlantic Margins. *J Earth Sci Climatic Change.* 2013. <https://doi.org/10.4172/2157-7617.S12-004>.
24. Ajama OD, Awoyemi MO, Arogundade AB, Dasho OA, Falade SC, Hammed OS, Shode OH. Deep crustal network of the Equatorial Atlantic fracture zones in southern Nigeria. *Results Geophys Sci.* 2021;8: 100027.
25. Blundell DJ. Active faults in West Africa. *Earth Planet Sci Lett.* 1976;31:287–90. [https://doi.org/10.1016/0012-821X\(76\)90221-1](https://doi.org/10.1016/0012-821X(76)90221-1).
26. Ajakaiye DE, Daniyan MA, Ojo SB, et al. The July 28, 1984 southwestern Nigeria earthquake and its implications for tectonics and evolution of Nigeria. *J Geodyn.* 1987;7:205–14. [https://doi.org/10.1016/0264-3707\(87\)90005-6](https://doi.org/10.1016/0264-3707(87)90005-6).
27. Lee DH, Ku CS, Yuan H. A study of the liquefaction risk potential at Yuanlin. *Taiwan Eng Geol.* 2004;71:97–117. [https://doi.org/10.1016/S0013-7952\(03\)00128-5](https://doi.org/10.1016/S0013-7952(03)00128-5).
28. Ulamis K, Kilic R. Liquefaction potential evaluation of the quaternary alluvium, Western Ankara (Turkey). *Environ Earth Sci.* 2012;67:945–58. <https://doi.org/10.1007/s12665-012-1526-1>.
29. Obaje NG. *Geology and mineral resources of Nigeria.* Berlin Heidelberg: Springer-Verlag; 2009. p. 219.
30. Oyedele KF, Meshida EA, Obidike CC. Assessment of coastal soil corrosivity using resistivity tomography at Lekki. Lagos, Nigeria. *Int J Sci Adv Technol.* 2012;2:77–81.
31. Jones HA, and Hockey RD. The geology of part of South-Western Nigeria. *Geological Survey of Nigeria Bulletin.* 31; 1964.
32. Adeoti L, Ojo AO, Adegbola RB, Fasakin OO. Geoelectric assessment as an aid to geotechnical investigation at a proposed residential development site in Ilubirin, Lagos, Southwestern Nigeria. *Arabian J Geosci.* 2016;9:1–10. <https://doi.org/10.1007/s12517-016-2334-9>.
33. Omatsola L, Adegoke OS. Tectonic evolution and cretaceous stratigraphy of Dahomey basin. *J Mining Geol.* 1981;18:130–7.
34. Park CB, Miller RD, Xia J. Multichannel analysis of surface waves. *Geophysics.* 1999;64(3):800–8.
35. Xia J, Miller RD, Park CB. Estimation of near-surface shear-wave velocity by inversion of Rayleigh wave. *Geophysics.* 1999;64:691–700.
36. Boulanger RW, Idris IM. CPT and SPT based liquefaction triggering procedures. Report UCD/CGM-14/01. Davis CA: University of California; 2004.
37. Idriss, I.M., and Boulanger, R.W. (2004). Semi-empirical procedures for evaluating liquefaction potential during earthquakes. In: 11th International conference on soil dynamics and earthquake engineering, and 3rd international conference on earthquake geotechnical engineering, Berkeley, 32–56. <https://doi.org/10.1016/j.soildyn.2004.11.023>.
38. Cubrinovski M, Ishihara K. Empirical correlation between SPT N-value and relative density for sandy soil. *Soil Foundation.* 1999;39:61–71. [https://doi.org/10.3208/sandf.39.5\\_61](https://doi.org/10.3208/sandf.39.5_61).
39. Terzaghi K, Peck RB. *Soil mechanics in engineering practice.* Wiley; 1948.
40. Alaneme KK, Okotete EA. Critical evaluation of seismic activities in Africa and curtailment policies—a review. *Geoenviron Disasters.* 2018;5:24. <https://doi.org/10.1186/s40677-018-0116-2>.
41. Thomas JE, George NJ, Ekanem AM, et al. Preliminary investigation of earth tremors using total electron content: a case study in parts of Nigeria. *NRIAG J Astron Geophys.* 2020;9:220–5. <https://doi.org/10.1080/20909977.2020.1723866>.
42. Hayati H, Andrus RD. Liquefaction potential map of Charleston, South Carolina based on the 1886 earthquake. *J Geotech Geoenviron Eng.* 2008;134:815–28. [https://doi.org/10.1061/\(ASCE\)1090-0241\(2008\)134:6\(815\)](https://doi.org/10.1061/(ASCE)1090-0241(2008)134:6(815)).
43. Ulusay R, Kuru T. 1998 Adana-Ceyhan (Turkey) earthquake and a preliminary microzonation based on liquefaction potential for Ceyhan town. *Nat Hazards.* 2004;32:59–88. <https://doi.org/10.1023/B:NHAZ.0000026790.71304.32>.
44. Iwasaki T. Soil liquefaction studies in Japan: state-of-the-Art. *Soil Dyn Earthq Eng.* 1986;5:2–70. [https://doi.org/10.1016/0267-7261\(86\)90024-2](https://doi.org/10.1016/0267-7261(86)90024-2).
45. Ishola KS, Amu B, Adeoti L. Evaluation of near-surface conditions for engineering site characterization using geophysical and geotechnical methods in Lagos, Southwestern Nigeria. *NRIAG J Astron Geophys.* 2022;11:237–56. <https://doi.org/10.1080/20909977.2022.2075160>.
46. Adegbola RB, Ayolabi EA, Allo W. Subsurface characterization using seismic refraction and surface wave methods: a case of Lagos state university, Ojo, Lagos state. *Arab J Geosci.* 2012. <https://doi.org/10.1007/s12517-102-0784-2>.
47. Kayen R, Moss R, Thompson, et al. Shearwave velocity-based probabilistic and deterministic assessment of seismic soil liquefaction potential. *J Geotech Geoenviron Eng.* 2013;139:407–19. [https://doi.org/10.1061/\(ASCE\)GT.1943-5606.0000743](https://doi.org/10.1061/(ASCE)GT.1943-5606.0000743).
48. Robertson PK. Evaluation of flow liquefaction and liquefied strength using the cone penetration test. *J Geotech Geoenviron Eng.* 2009;136:842–53. [https://doi.org/10.1061/\(ASCE\)GT.1943-5606.0000286](https://doi.org/10.1061/(ASCE)GT.1943-5606.0000286).
49. Maurer BW, Green RA, Cubrinovski M, Bradley BA. Evaluation of the liquefaction potential index for assessing liquefaction hazard in Christchurch, New Zealand. *J Geotech Geoenviron Eng.* 2014;140:04014032. [https://doi.org/10.1061/\(ASCE\)GT.1943-5606.0001117](https://doi.org/10.1061/(ASCE)GT.1943-5606.0001117).
50. Andrus RD, Stokoe KHIII. Liquefaction resistance of soils from shear-wave velocity. *J Geotech Geoenviron Eng.* 2000;126:1015–25. [https://doi.org/10.1061/\(ASCE\)1090-0241\(2000\)126:11\(1015\)](https://doi.org/10.1061/(ASCE)1090-0241(2000)126:11(1015)).